Published by
NIGERIAN SOCIETY OF PHYSICAL SCIENCES
Available online @ https://journal.nsps.org.ng/index.php/jnsps

J. Nig. Soc. Phys. Sci. 5 (2023) 1183

Journal of the Nigerian Society of Physical Sciences

Effects of different electrolytes on the structure and yield of graphene oxide produced via electrochemical exfoliation

O. D. Adigun[a,b,*], L. E Umoru[b], T. N. Iwatan[a]

[a]*Department of Materials and Metallurgical Engineering, Federal University Oye Ekiti, Nigeria*
[b]*Department of Materials Science and Engineering, Obafemi Awolowo University, Ile-Ife, Nigeria*

Abstract

The most suitable electrolyte for graphene oxide synthesis, in terms of both production efficiency and quality, using the electrochemical exfoliation technique has been investigated and reported in this study. Simultaneous anodic and cathodic graphene oxide production using ten (10) different electrolytes, including acids (H_2SO_4, HCl, HNO_3), bases (KOH, $Ca(OH)_2$, $Mg(OH)_2$, NaOH), and salts (NaCl, $(NH_4)_2SO_4$, K_2SO_4), was studied under the same experimental conditions of bias voltage, graphite nature, exfoliation time, electrolyte molarity, and post-exfoliation treatments. Assessment of the graphene oxide structures and production rates was supported using Raman spectroscopy, high-resolution scanning electron microscopy (HRSEM), and EDS (energy dispersive x-ray spectroscopy), attached to the scanning electron microscope. Analysis of the results obtained reveals that H_2SO_4 showed the highest graphene oxide yield (86%) but with comparably low graphene oxide quality in terms of defect concentration, presence of oxygen functional group contamination, and crystallite properties. The aqueous NaCl, $Ca(OH)_2$ and $Mg(OH)_2$ electrolytes did not show any graphene oxide exfoliation effect. However, from the series of electrolytes examined, aqueous $(NH_4)_2SO_4$ exhibited an excellent combination of efficient graphene oxide yield and high-quality characteristics due to its relatively high yield of 74% and superior quality of the produced graphene oxide with the comparatively lowest defect density, η_D, and highest C/O (carbon-to-oxygen) ratio. The tortuous, agglomerated, and planar layers of the distinct 2D graphene oxide sheets were also clearly revealed by the SEM images. In essence, the roles played by dissociated sulfate (SO_4^{2-}), nitrate (NO_3^{2-}), chlorides (Cl^-), and hydroxides (OH^-) ions in the series of complex electrochemical reactions toward the intercalation, exfoliation, yield, and properties of graphene oxide produced are discussed. From the series of electrolytes tested, aqueous $(NH_4)_2SO_4$ emerged as the most relatively suitable electrolyte for the synthesis of graphene oxide because it combines both high yield and fine quality.

DOI:10.46481/jnsps.2023.1183

Keywords: Graphene oxide, electrochemical exfoliation, electrolytes, quality, yield or production rate, graphite

Article History :
Received: 07 November 2022
Received in revised form: 11 September 2023
Accepted for publication: 13 September 2023
Published: 12 October 2023

Communicated by: B. J. Falaye

1. Introduction

Graphene is a recent and famous nanomaterial of carbon origin with a two-dimensional hexagonal (honeycomb) lattice structure stacked in monolayers of carbon atoms [1]. It has exceptional mechanical [2], electrical/electronic [3], optical [4], and thermal [5] properties that give it vast opportunities (both as a free building block or additive) as an outstanding candidate for the next generation of state-of-the-art technologies in various areas, including medical [6], energy storage [7, 8], sen-

*Corresponding author tel. no: +2348039151934
Email address: oluwole.adigun@fuoye.edu.ng (O. D. Adigun)

sors, e.g., microelectromechanical systems (MEMS) [9], civil construction [10], etc.

However, one of the current challenges with the execution of its benefits in end-use applications is related to the difficulty of its mass production. In essence, due to the relevance of graphene-containing materials to future technological revolutions in various fields, the growing need to improve on the current state of its production has been on the rise in recent years, and attempts to overcome the challenges aimed at devising a cost-effective approach for the synthesis of high-quality graphene capable of high yield have been a subject of discussion over time [11, 12]. Among the various protocols through which graphene can be synthesized, the electrochemical exfoliation method has been identified as capable of mass production [13].

The mechanism behind the electrochemical exfoliation of graphite for graphene synthesis depends on the effective intercalation of the electrolyte ions in between the tiny interlayers and the ensuing gas-inflated scaling off of the flakes [14]. The electrolyte ions preferentially bombard the hybridized carbon atoms at the edge sites and grain boundaries to intrude between and weaken the lattice sequence, creating room for the gas-enabled exfoliation of the graphite sheets for further treatments into graphene [15]. Hence, while the radical and ionic species intercalate the graphite electrodes through the edge sites and grain boundary, the gaseous species promote volume expansion that leads to flaking. For systems where the cathode and anode are both graphite, intercalation and exfoliation may occur simultaneously at both electrodes [16].

Studies have shown that the rate of shearing is faster at the anode than at the cathode due to the role played by the anions as well as oxygen-based free radicals [17]. While the anodic process involves a fast, high yield, and highly crystalline graphene product with mono- to few-layer structure, cathodic exfoliation is associated with drawbacks such as: i) an extremely low and slow exfoliation yield. ii) small lateral sizes of the flake; and iii) post-treatment of the flake requires a longer sonication time in order to ensure complete exfoliation [18]. As a result of this, some studies are based only on the anodic exfoliation process [11]. However, a system consisting of both cathodic and anodic processes may retain a higher overall yield over the sole anodic exfoliation approach. Moreover, intercalation and exfoliation yield efficiency also depend on factors like the redox potential and activities of the free radicals or ionic species present [14, 19, 20].

The high yield associated with the use of aqueous H_2SO_4 as an electrolyte in the electrochemical exfoliation of graphene has been revealed and identified as instrumental to the mass production of graphene [21, 22]. However, the drawback of the use of sulfuric acid (H_2SO_4) comes from the associated high O/C (oxygen to carbon) ratio and low structural quality of the graphene [23], and the use of sulfate salts in lieu of the acid has been studied by researchers with different outcomes [24]. Likewise, halide electrolytes were recently proposed as a way out of the high oxygen contamination, but intercalation by the halide ions resulted in a very low yield [25].

Current developments have also devised a means to reduce the high O/C ratio generated by the oxygen functional group released from the sulfate radical (SO_4^-) by the addition of additives, but the resulting structure of the produced graphene needs to be further investigated [14, 26, 27]. Consequently, no single method is currently available that could simultaneously produce a high yield of graphene oxide with good quality and at a low cost [25]. In a bid to optimize the electrochemical exfoliation process of graphene oxide production, various studies have erupted with the use of different electrolytes, with various levels of success [24]. But these were achieved under different experimental conditions that make an effective comparison of the yield and structure of the produced graphene oxide less accurate.

Some of these inconsistent experimental conditions include: exfoliation time, applied voltage, nature of graphite electrodes employed (i.e., foil, sheet, rod, HOPG-highly oriented pyrolytic graphite, etc.), sonication time, volume of graphite electrode immersed in the electrolyte, molarity, etc. [28–30]. This may have led to conflicting reports over the years. In spite of the achievements so far recorded, recommendations on the finest combination of electrolytes and synthetic parameters for an efficient rate of production, a good graphene oxide finish, and process walkability are still missing. Yet, the need to converge the available progress in order to work out a definite selection of the relatively most suitable electrolyte that could combine cost effectiveness with efficient yield and structural stability is hampered by the different experimental conditions in which the various studies have so far been carried out.

Apparently, no accurate convergence of the currently available information can be made without a panoramic investigation that could subject the series of electrolytes to the same experimental conditions for a prolific correlation of their strengths and weaknesses towards a reasonable recommendation of the most suitable electrolyte capable of optimum capacity that could combine effective cost with competent yield and the fine quality of the produced graphene oxide.

This study investigated the productive capacity and structure of electrochemically exfoliated graphene oxide using different electrolytes, including nitric acid (HNO_3), sulfuric acid (H_2SO_4), hydrochloric acid (HCl), potassium hydroxide (KOH), calcium hydroxide ($Ca(OH)_2$), magnesium hydroxide ($Mg(OH)_2$), sodium hydroxide (NaOH), sodium chloride (NaCl), ammonium sulfate ($(NH_4)_2SO_4$), and potassium sulfate K_2SO_4. Structure, morphology, and defect characterization of the graphene oxide synthesized from the different electrolytes were determined using Raman spectroscopy, a high-resolution scanning electron microscope (HR-SEM), and EDS (energy dispersive x-ray spectroscopy) attached to the scanning electron microscope. The roles of the associated oxide and non-oxide radicals and ionic species towards the intercalation and exfoliation of the produced graphene oxide were evaluated with a view to assessing their influence on both yield efficiency and the overall graphene oxide structure. These were corroborated with the analysis of the morphology and chemical composition of the synthesized graphene oxides. The study provides a wider scope of evaluation made up of a selection of ten electrolytes subjected to the same graphene oxide synthesis method

and uniform experimental conditions in order to ensure efficient optimization of the electrolyte-selection process towards the finest combination of both yield and quality of the produced graphene oxide. Therefore, the series of synthesises were subjected to the same experimental conditions of exfoliation time (100 minutes), applied voltage (12 V), nature of graphite electrodes employed (graphite rod), sonication time (120 minutes), and molarity (0.2 M). In order to maximize the graphene oxide flake yield, the anodic/cathodic exfoliation route has been adopted, using graphite as both the anode and the cathode electrodes, and the yield of graphene oxide is examined from the mass of delaminated flakes at the cathode and anode. The preferential roles played by the dissociated sulfate (SO_4^{2-}), nitrate (NO_3^{2-}), chlorides (Cl^-), and hydroxides (OH^-) ions; the oxygen radicals (HO^-, SO_4^{2-} and NO_2^-); associated gases; as well as the non-oxide radicals (NH_3, NH_2, and NH) in the aqueous electrolyte solutions towards the intercalation, exfoliation, yield, and properties of graphene oxide produced were investigated and presented.

2. Experiment and Method

Graphite rods that were collected from waste lithium ion batteries were used as both the anode and cathode in the electrochemical set-up. Aqueous solutions of the bases and salt electrolytes were prepared in a beaker by dissolving the weighted solute in distilled water and making up the solution to the mark in a volumetric flask via the addition of distilled water to obtain the desired concentration of 0.2 M. For the acid electrolytes, the calculated volume of stock solution is measured using a measuring cylinder before being transferred into a volumetric flask containing an amount of distilled water and being made up to the desired concentration of 0.2 M by the addition of more distilled water. The graphite rods were thoroughly cleaned with distilled water and air-dried before taking their initial dimensions and weight. The electrochemical set-up is made using a jumper cable connected to a DC supply, a 250-ml beaker, and an alligator clip in the presence of individual electrolytes and the graphite electrodes.

A potential difference of 12 V is simultaneously applied to each set-up for 100 minutes to achieve the electrochemical delamination of the flake before the post-exfoliation treatments. Meanwhile, the experimental conditions were kept constant, and only the electrolytes were different. For the electrolytes that showed exfoliation effects, the delaminated flake could be seen moving randomly within the solution, while the electrolytes with no visible exfoliation effects remained still throughout the exfoliation time.

Afterwards, the flake-electrolyte mixture is transferred to a 20-ml tube for separation using a centrifuge machine (Model 800D: 6 × 20-ml holes). Washing with acetone and collection in the designated sample bottles are also done before drying in the laboratory oven at 50 ^oC. The dried flake is then subjected to the post-exfoliation treatments by dissolution in a solution of distilled water combined with acetone in the ratio 4:1 and sonication for 2 hours in an ultrasonic bath holding deionized water (Sororex Super RK 514 BH, Bandelin). The mixture is then dried using a hot, air-circulating laboratory oven at 100 °C for 2 hours. The characterization of the produced materials is buttressed using a high-resolution scanning electron microscope, HR-SEM (Philips XL30 FEG, USA), Raman spectroscopy (HR Raman Spectroscope HR800, Horiba Jobin Yvon GmbH) and energy dispersive x-ray spectroscopy (EDS) attached to the scanning electron microscope.

3. Results and Discussion

3.1. The role of electrolytes' ionic species towards the graphene oxide yield

Among the various aqueous solutions of acid, base, and salt electrolytes investigated, the sulfate electrolytes showed the best graphene oxide exfoliation yield, with H_2SO_4 exhibiting the highest yield (86%), followed by $(NH_4)_2SO_4$ and K_2SO_4 with 74% yield each, before the other electrolytes. The tested sulfate electrolytes are aqueous forms of H_2SO_4, $(NH_4)_2SO_4$, and K_2SO_4, but it is the aqueous $(NH_4)_2SO_4$ electrolyte that displayed the finest quality of the graphene oxide produced among all the tested electrolytes (in terms of crystallite structure, defect concentration, and inter-defect distance).

The mechanism for graphene oxide delamination during the electrochemical exfoliation involves intercalation (which results in soaking and expansion of the layered structure of the graphite), oxidation (for the anodic exfoliation), reduction (for the cathodic exfoliation), gaseous emission, and subsequent exfoliation [31]. The higher intercalation efficiency shown by the sulfate-containing electrolytes has been linked to the larger ionic size of the SO_4^{2-} ion (0.46 nm) than the interlayer distance between stacked graphite sheets (0.34 nm) that helps propel initial expansion [32]. In addition, the higher oxidation potential of the sulfate radical (SO_4^-= +2.6 V) that is triggered by the water-to-graphite interface over the applied voltage may have assisted the intercalation process. Similarly, the oxidation potential of the hydroxyl radical HO is +2.8 V [1]. The combined strength of the oxidation potentials of the HO and SO_4 radicals generates a high propensity for electron loss and oxidation that attack the graphite anode at the grain boundary or edges, and this is crucial to the intercalation of the graphite *d*-spacing [33–35]. Consequently, large streams of gas bubbles such as SO_2, H_2, CO_2, CO, and O_2 were generated at the anode/cathode -electrolyte interface by the sophisticated electrochemical reactions that exerted pressure in-between the graphite layers to propel exfoliation of the graphene oxide sheets [36].

Information about the detection and flow rate of these gases has been reported in a different study [37]. As the exfoliation proceeds, the generated gas bubbles can be visibly observed at the electrode-electrolyte interface, and the evolution of the gases causes a noticeable reduction in the volume of the electrolyte in accordance with the law of conservation of mass. Also, the dispersion of the delaminated graphene oxide sheets in the electrolyte is perceived by the random movement of the exfoliated particles in the solution. While attack by the oxygen-containing radicals could be beneficial to intercalation and invariably graphene oxide yield, the synthesized products were

contaminated by the allied oxygen functional groups, and this affected the ensuing quality of the graphene oxide [27]. However, the problem of high O/C ratios associated with sulfate-ion-containing electrolytes has been contained by the use of additives and anti-oxidation agents, as revealed in recent publications [14, 26, 27]. Moreover, a thermal post-exfoliation treatment could be employed to decompose the oxygen functional groups in order to release the corresponding oxygen gases for better graphene quality.

Similar to the sulfate electrolytes, the aqueous nitric acid HNO_3 showed a yield of 70%, which could be attributed to the activities of the generated nitrogen dioxide radical, NO_2, that aided the anodic intercalation process while the associated gases (NO_x, H_2, CO_2, CO, and O_2) enabled the delamination of the graphene oxide flake. Also, the NO radical has been reported to produce O functional groups that equally affect the quality of graphene oxide [24].

Furthermore, by assessing the suitability of aqueous solutions of some common bases (KOH, $Ca(OH)_2$, $Mg(OH)_2$, and NaOH) as electrolytes for the simultaneous anodic and cathodic exfoliation of graphene oxide from the graphite rods, it is observed that only KOH and NaOH show exfoliation effects with approximately 25% yield each, while $Ca(OH)_2$ and $Mg(OH)_2$ showed no exfoliation effect at the electrodes. It is also observed that no gas bubbles were generated within the set-ups containing the aqueous $Ca(OH)_2$ and $Mg(OH)_2$ electrolytes, as they remained still throughout the exfoliation time. The behavior of these strong and weak bases could be described by their tendencies to ionize in water.

Both KOH and NaOH are strong bases that ionize completely in water to completely disengage their ions in the solution for the electrochemical reactions, while $Ca(OH)_2$ and $Mg(OH)_2$ are weak bases that are made up of a large number of base molecules that remain undissociated. The uniformly adopted molarity of 0.2 M for the series of tested electrolytes may also be too low to propel dissociation of the $Ca(OH)_2$ and $Mg(OH)_2$ solutions for any possible exfoliation effect. Therefore, it is the OH^- ions of the strong base that get dissociated for the intercalation and exfoliation of the graphite flakes. Hence, both KOH and NaOH show a 25% exfoliation yield, while the weak bases (i.e., $Ca(OH)_2$ and $Mg(OH)_2$) show no traces of intercalation or exfoliation of the graphite electrodes. As much as the weak bases may be ruled out for electrochemical exfoliation of graphene oxide purposes, the strong bases may not be better off due to their relatively low exfoliation yield tendencies.

For the halide electrolytes examined (i.e. HCl and NaCl), a 40% exfoliation yield was noticed for the dilute HCl solution, while NaCl showed no exfoliation effect. Halide salt electrolytes (including NaCl) have been recently linked with the anodic exfoliated production of single- to few-layer graphene oxide with a lower O/C ratio than that obtained from frequently used electrolytes like H_2SO_4 [25]. However, the ease with which the aqueous halide salts yielded the graphene oxide flake using a graphite foil electrode in the study by Munuera (2017) may be distinctly different from the situation with a graphite rod electrode (this work) that is *ab initio* produced by the compression of natural graphite under high pressure, as this could retard the ease with which delamination of the graphene oxide flakes may occur [25].

Over time, the tendency of halide ions to intercalate or exfoliate graphite for graphene oxide synthesis has been greased with mixed reactions. While some studies reveal that halide salt electrolytes do not show any exfoliation results [23, 29, 37], a few others report the capability of halide electrolytes to exfoliate graphene oxide [1, 25]. Experimental conditions such as the nature of the graphite employed, the long exfoliation time, the use of high voltage bias, etc. may have contributed to the disparities in the results. In essence, further investigation of the exfoliation effects of halide electrolytes is still required in order to explain the contradictions in their reported exfoliation outcomes.

3.2. *Structure and defect concentration of the graphene oxides produced by the electrolytes*

The structure of graphene oxide produced by the different electrolytes is investigated using Raman spectroscopy, achieved by the adoption of a uniform excitation laser of 514.5 nm across all the samples. Raman spectroscopy is a non-destructive vibrational technique that is almost indispensable in the study of macro, micro, or nano carbon materials because it reveals the bonding, defects, and geometric structure [38, 39]. The Raman spectra of graphene oxide show characteristic principal bands denoted as 2D, G, and D bands with significant differences in their relative intensities and shape profiles (see Figure 1).

The G band is an in-plane mode associated with the sp^2 hybridized carbon network of the graphene oxide material; the D band is a resonated ring breathing mode that represents disorder or defect proportion from the edge-position of the sp^2 carbon rings; and the 2D band is a two-phonon lattice vibrational mode that represents a second-order overtone of the D band devoid of associated defects [38]. Over the years, analysis of these bands has provided useful insights into the structure of graphene oxide materials. Also, there are possibilities of associated Raman spectra such as the 2D', D+G, and D' bands that supply useful complementary information [40]. For the tested electrolytes, the D bands were observed at ~1356-1361 cm^{-1}, the G bands at ~1585-1595 cm^{-1}, and the 2D bands are shown at ~2700 - 2717 cm^{-1} as shown in Figure 1. These observations conform with the literature's Raman shifts for the respective D, G, and 2D bands of graphitic materials [41–43].

The integrated intensity ratio of the D and G bands (A_D/A_G) of the Raman spectra is used to investigate the structure of the synthesized graphene oxide materials via Eqs. (1)–(4). Evaluation of the lateral crystallite size, L_a, is done using Eq. (1) [44], where λ is the laser line wavelength used (5.14.5 nm).

$$L_a = \frac{(2.4 \times 10^{-10})\lambda_L^4}{A_{D/}A_G} \tag{1}$$

$$L_{eq} = 33.6343\frac{A_{2D}}{A_G} \tag{2}$$

Figure 2a shows the lateral crystallite size, L_a, for the synthesized graphene oxide materials from the different electrolytes.

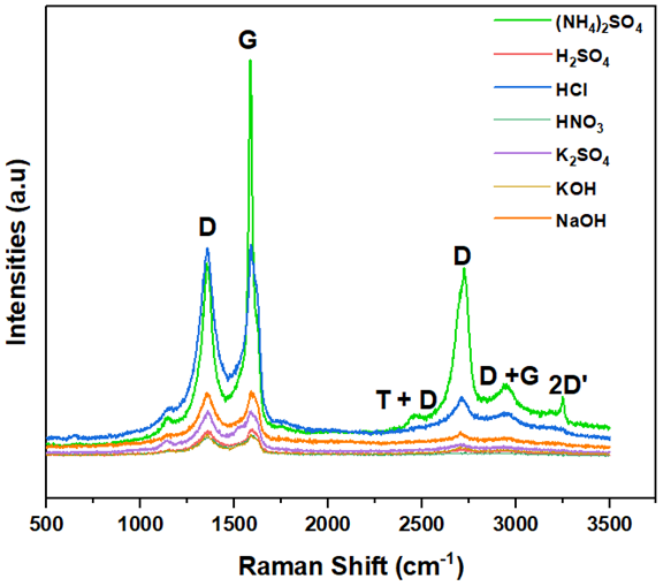

Figure 1. Raman spectra of electrochemically exfoliated graphene oxide synthesized using different electrolytes under the same experimental conditions (NaCl, $Ca(OH)_2$, and $Mg(OH)_2$ show no exfoliation effect)

Accordingly, the electrolytes that did not show any exfoliation effect (i.e., NaCl, $Ca(OH)_2$, and $Mg(OH)_2$) were excluded from the chart. It can be seen from Figure 2a that the graphene oxide synthesized using $(NH_4)_2SO_4$ revealed superior structural stability in terms of the comparatively largest lateral crystallite size, L_a. Generally, a small L_a size may be attributed to structural disorder and flaws traceable to: the presence of edges in the stacking layers of the synthesized graphene oxide; nonconformity of the graphene oxide layer planarity; and the presence of amorphous carbon species in sp^3 hybridized form [45]. Moreover, in a study by Parvez and his colleagues [29], the graphene oxide produced using aqueous $(NH_4)_2SO_4$ equally showed superior quality among the three electrolytes tested (i.e. aqueous $(NH_4)_2SO_4$, K_2SO_4 and Na_2SO_4). Besides, Larouch and Stansfield reported that a parameter called the average continuous graphene length including tortuosity, L_{eq}, is a better measure for the investigation of the nanostructure in graphitic carbons than the lateral crystallite size, L_a [46]. Therefore, the continuous graphene length, including tortuosity, L_{eq}, of the synthesized samples is determined by the product of tortuosity ratio ($R_{Tor} = 2A_{2D}/A_G$) and L_a, and can be calculated as presented in Eq. (2).

Figure 2b reports the average continuous graphene length, including tortuosity, L_{eq}, of the synthesized samples. It has also been reported that a higher L_{eq} is proportional to a higher crystalline quality. The synergy between L_a and L_{eq} is such that: $L_{eq} > L_a$ is an indication of the presence of curved and lengthy layers (tortuosity), and the small planar units can be well connected within the structure; and $L_{eq} = L_a$ indicates that the graphene layers are short and planar. Among the graphene oxide materials synthesized using the various electrolytes, the presence of tortuosity in the graphene oxide synthesized by the aqueous $(NH_4)_2SO_4$ could be clearly deduced, as supported by Figures 2a and 2b. Also, the samples synthesized from the other tested electrolytes show various levels of the presence of small and planar graphene layers (samples synthesized using HNO_3, K_2SO_4, and NaOH) to the absence of tortuosity (for samples synthesized using H_2SO_4, HCl, and KOH). The efficiency of aqueous $(NH_4)_2SO_4$ electrolyte for the mass production of high-quality graphene could, therefore, be possible considering its recorded promising yield (74%). Consequently, the larger lateral crystallite size as well as the presence of tortuosity in the graphene oxide synthesized using an aqueous $(NH_4)_2SO_4$ electrolyte are promising for exceptional electrical, optical, and mechanical properties [47]. Furthermore, the superior structural qualities displayed by the graphene oxide synthesized using aqueous $(NH_4)_2SO_4$ can be attributed to the nitrogen doping tendency of the electrolyte. Hetero or monoatomic doping of graphene oxide may simultaneously occur during electrochemical exfoliation of graphite. Using aqueous $(NH_4)_2SO_4$ as the electrolyte, the electrochemical exfoliation process in a series of complex reactions generated a series of nitrogen-based radicals such as NH_3, NH_2 and NH that reacted with the produced flake to form N-doped graphene oxide [24]. Meanwhile, N-doped graphene oxide exhibits a more excellent electrocatalytic tendency towards oxygen reduction that helps modulate the structure of the materials, besides other fascinating features like better catalytic properties, improved conductivity, higher photoelectrochemical characteristics, etc. [48, 49].

The presence of defects is considered detrimental to useful intrinsic properties in graphene and graphene-based materials [50]. Structural flaws in the synthesized graphene oxide materials are further inferred by the defect density, η_D and inter-defect distance using Eqs. (3) and (4), respectively, in line with the submission of Cançado *et al.* [40].

$$\eta_D = \frac{2.4 \times 10^{22}}{\eta_L^4}\left(\frac{A_D}{A_G}\right), \tag{3}$$

$$L_D = \sqrt{(1.8\ x\ 10{-}9)\eta_L^4\left(\frac{A_G}{A_D}\right)}. \tag{4}$$

Structural defects in graphene oxide are created during the electrochemical exfoliation process by chemical functionalization through the inherent functional groups [51]. The concentration of the defect density and the inter-defect distance of the graphene oxide produced by the selected series of electrolytes are presented in Figures 2c and 2d, respectively. Among the tested samples, the results reveal that the graphene oxide synthesized using an aqueous solution of H_2SO_4 has comparatively the poorest defect structure by showing the relatively highest defect density, η_D, of $5.2 \times 10^{11}cm^{-2}$ (see Figure 2c) and the lowest inter-defect distance, L_D, of 9.1 nm (see Figure 2d). Note that the value of the worst-case defect density, η_D, shown by the graphene oxide produced using the aqueous H_2SO_4 (in this work) is however better than that shown by a totally disordered graphene with η_D value of $\sim\times 10^{15}cm^{-2}$ [19]. On the other hand, the finest defect structure is displayed by the graphene oxide produced using the aqueous solution of $(NH_4)_2SO_4$ with the combination of the relatively lowest and highest defect density and inter-defect distance, respectively.

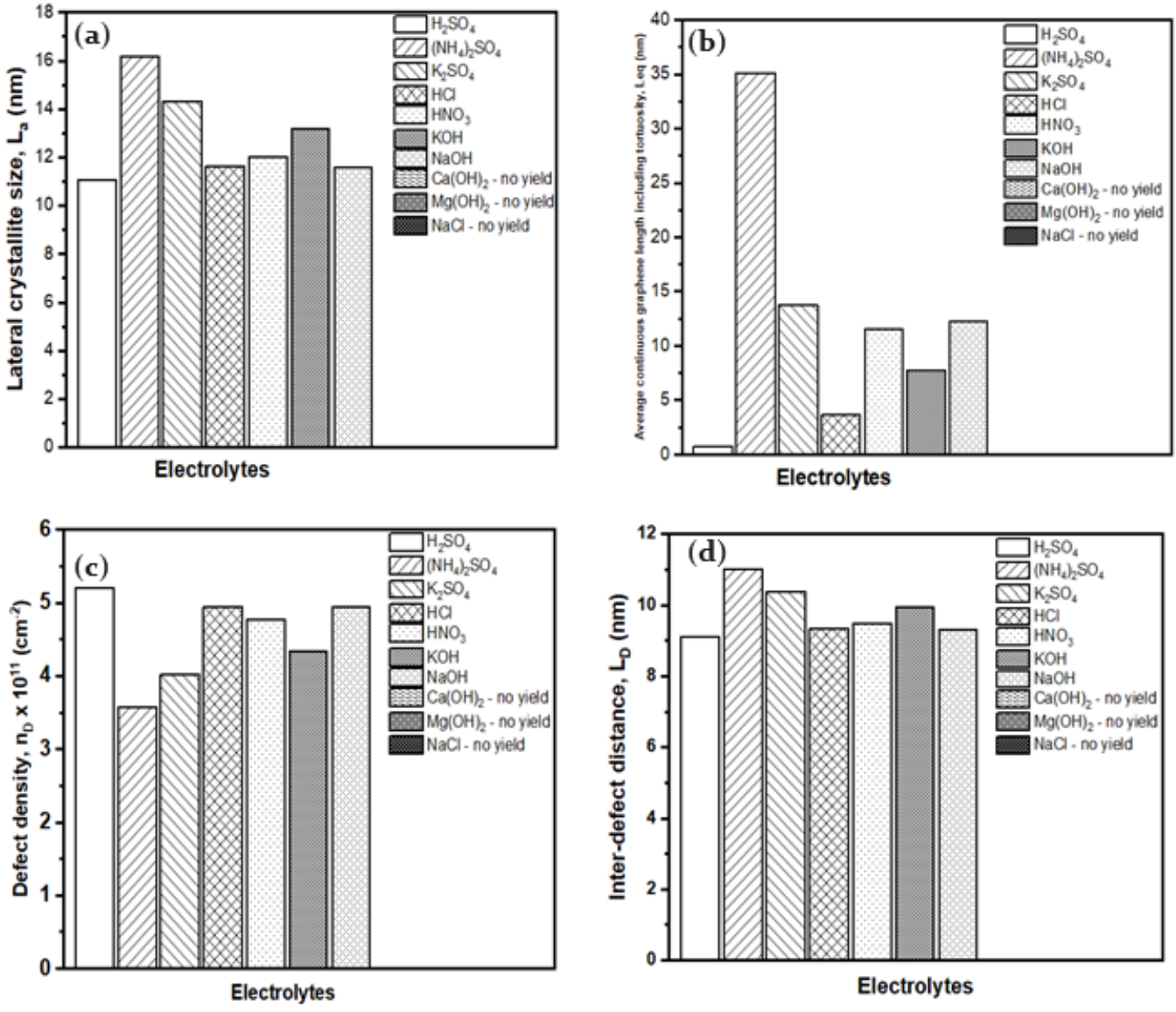

Figure 2. Analysis of the structure and defects of the graphene oxide produced by the different electrolytes: a) Analysis of the lateral crystallite size, L_a; b) Analysis of the average continuous graphene length including totuosity, L_{eq}; c) Analysis of the defect density, η_D d) Analysis of the inter-defect distance, L_D

3.3. Morphology and chemical composition of the produced graphene oxides

A high-resolution scanning electron microscope (HR-SEM) was used to study the morphology of the synthesized graphene oxides. SEM images of the graphene oxides generally indicate a layered structure, where the edges of the layers look crumpled or folded. The morphology of graphene oxide varies slightly with the electrolytes employed in the electrochemical exfoliation process, and this may be attributed to the varying degrees of oxidation and C/O ratios. The morphology equally shows the presence of wrinkles and folds in the graphene sheets (see Figure 3a-c). The graphene oxide structure assessed using Raman spectroscopy as described in Section 3.2 is corroborated from the SEM images by the irregular folding, wrinkles, planar, and stretching layers of the sheets. Consequently, the highly tortuous graphene oxide produced using $(NH_4)_2SO_4$, as characterized by the average continuous graphene length including tortuosity, L_{eq}, is supported from the SEM images by the wrinkles and stretching appearance (see Figure 3a).

Energy dispersive x-ray spectroscopy (EDS) attached to the high-resolution scanning electron microscope (SEM) was used to investigate the chemical composition of the graphene oxides exfoliated by the different electrolytes and presented in Table 1. A very close margin of C/O ratio is observed among the graphene oxide samples. The graphene oxide samples synthesized using $(NH_4)_2SO_4$ showed the comparatively highest C/O ratio, while those synthesized using H_2SO_4 presented the lowest C/O ratio. Basically, the performance of graphene oxide is retarded by the oxygen functional group [51]. In essence, the functional stability of the graphene oxide is propelled by in-

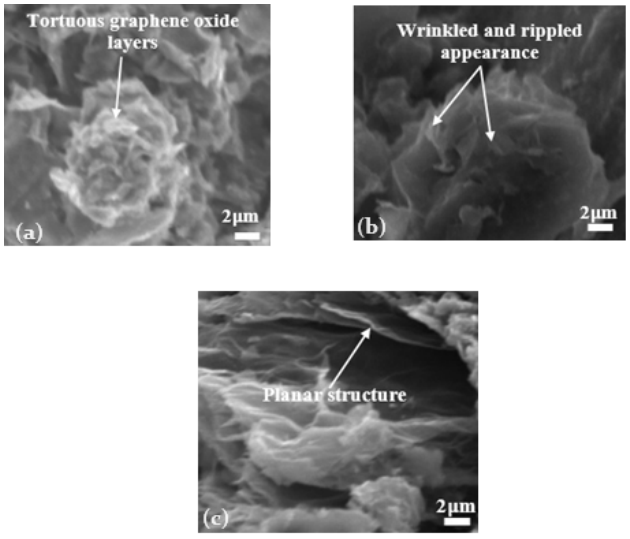

Figure 3. Figure 3: SEM images of some of the synthesized graphene oxides: a) SEM image of the graphene oxide synthesized using the aqueous $(NH_4)_2SO_4$; b) SEM image of the graphene oxide synthesized using the aqueous H_2SO_4; c) SEM image of the graphene oxide synthesized using the aqueous HNO_3.

Table 1. Structure and chemical composition of the synthesized graphene oxide materials

Electrolytes	Stacking of the graphene oxide		C/O ratio
	I_g/I_{2d}	Number of layer	
$(NH_4)_2SO_4$	0.584	1-3 layer	3.91
H_2SO_4	0.588	1-3 layer	2.62
K_2SO_4	0.587	1-3 layer	3.55
HNO_3	0.587	1-3 layer	3.55
HCl	0.588	1-3 layer	3.89
NaOH	0.588	1-3 layer	3.89
KOH	0.587	1-3 layer	3.26

creasing the C/O ratio, and a higher C/O ratio could give a better quality. The relatively high C/O ratio observed in the graphene oxide produced using the aqueous $(NH_4)_2SO_4$ solution may be attributed to the dissociation of the ionic species during the electrochemical reaction that causes nitrogen doping of the exfoliated graphene oxide and the evolution or replacement of some oxygen functionalities. On the other hand, different studies confirmed the associated high oxygen content in graphene oxide synthesized using H_2SO_4 [27]. The dissociated ionic species in the aqueous solutions apparently influenced the C/O ratio in the graphene oxide produced by each of the electrolytes and subsequently the functional stabilities.

4. Conclusion

The efficiency of different electrolytes for the electrochemical exfoliation of graphene oxide in terms of both yield and quality from a selected series of aqueous sulfates, nitrates, chlorides, and hydroxides comprising acids, bases, and salts has been investigated in this study. The tested electrolytes, i.e., H_2SO_4, HCl, HNO_3, KOH, $Ca(OH)_2$, $Mg(OH)_2$, NaOH, NaCl, $(NH_4)_2SO_4$, and K_2SO_4, were examined under the same experimental conditions of voltage bias, exfoliation time, sonication time, molar concentration, etc., for the graphene oxide synthesis and the characterization done using Raman spectroscopy, high-resolution scanning electron microscopy (HR-SEM), and energy dispersive x-ray spectroscopy (EDS) attached to the scanning electron microscope. Among the various aqueous solutions of acids, bases, and salt electrolytes investigated, sulfate electrolytes showed the best graphene oxide exfoliation yield, with H_2SO_4 exhibiting the highest yield (86%), followed by $(NH_4)_2SO_4$, and K_2SO_4 with 74% yield each, but $Ca(OH)_2$, $Mg(OH)_2$, and NaCl showed no exfoliation effect, i.e., without any graphene oxide yield. Consequently, the graphene oxide produced using $(NH_4)_2SO_4$ displayed the finest structural quality among all the tested ten (10) electrolytes in terms of structural stability and level of imperfections or defects. The complex physicochemical changes that led to the very high yield of the aqueous sulfate electrolytes and the superior quality shown by the graphene oxide material produced using the $(NH_4)_2SO_4$ is attributed to:

- the combined force of the oxidation potentials of the HO and SO_4^- radicals that generated a very high propensity for electron loss and oxidation to intercalate the graphite electrode at the grain boundaries or edges;
- the large stream of gas bubbles (SO_2, H_2, CO_2, CO, O_2) generated at the electrode -electrolyte interface by the sophisticated electrochemical reactions that exerts pressure in-between the graphite layers to propel delamination of the graphene oxide sheets;
- the nitrogen doping tendency of the aqueous $(NH_4)_2SO_4$ electrolyte to simultaneously produce N-doped graphene oxide during the electrochemical exfoliation process with the help of associated nitrogen-based radicals such as NH_3, NH_2 and NH; that facilitates the fascinating properties exhibited by the N-doped graphene materials including low defect concentration and the removal of the oxygen functional groups, leading to a higher value of the C/O ratio.

On account of the high yield and exceptional quality in terms of structural stability and defect level, aqueous $(NH_4)_2SO_4$ may be preferentially considered for the mass production of graphene using the electrochemical exfoliation technique.

Acknowledgment

We thank the referees for the positive enlightening comments and suggestions, which have greatly helped us in making improvements to this paper.

References

[1] X. Wang & L. Zhang, "Green and facile production of high-quality graphene from graphite by the combination of hydroxyl radicals and electrical exfoliation in different electrolyte systems" RSC Advances **9** (2019) 3693. https://doi.org/10.1039/c8ra09752f.

[2] J. Wang, X. Jin, C. Li, W. Wang, H. Wu & S. Guo, "Graphene and graphene derivatives toughening polymers: Toward high toughness and strength", Chemical Engineering Journal **370** (2019) 851. https://doi.org/10.1016/j.cej.2019.03.229.

[3] C. Shen, J. E. Calderon, E. Barrios, M. Soliman, A. Khater, A. Jeyaranjan, L. Tetard, A. Gordon, S. Seal & L. Zhai, "Anisotropic electrical conductivity in polymer derived ceramics induced by graphene aerogels", Journal of Materials Chemistry C **5** (2017) 11708. https://doi.org/10.1039/c7tc03846a.

[4] M. Li, T. Chen, J. J. Gooding & J. Liu, "Review of carbon and graphene quantum dots for sensing", ACS Sensor **4** (2019) 1732. https://doi.org/10.1021/acssensors.9b00514.

[5] D. Li, Z. Yang, D. Jia, D. Wu, Q. Zhu, B. Liang, S. Wang & Zhou, "Microstructure, oxidation and thermal shock resistance of graphene reinforced SiBCN ceramics", Ceramics International **42** (2016) 4429. http://dx.doi.org/10.1016/j.ceramint.2015.11.127.

[6] J. Shen, Y. Zhu, X. Yang & C. Li, "Graphene quantum dots: emergent nanolights for bioimaging, sensors, catalysis and photovoltaic devices", Chemical communications (Cambridge, England) **48** (2012) 3686. https://doi.org/10.1039/c2cc00110a.

[7] Y. Ren, B. Yang, X. Huang, F. Chu, J. Qiu & J. Ding, "Intercalated SiOC/graphene composites as anode material for li-ion batteries", Solid State Ionics **278** (2015) 198. http://dx.doi.org/10.1016/j.ssi.2015.06.020.

[8] S. O. Bolarinwa, E. Danladi, A. Ichoja, M. Y. Onimisia & C. U. Achem, "Synergistic study of reduced graphene oxide as interfacial buffer layer in HTL-free perovskite solar cells with carbon electrode", Journal of the Nigerian Society of Physical Sciences **4** (2022) 909. https://doi.org/10.46481/jnsps.2022.909

[9] Q. Wang, Y. Wang & L. Dong, "MEMS flow sensor using suspended graphene diaphragm with microhole arrays" Journal of Microelectromechanical Systems **27** (2018) 951. https://doi.org/10.1109/JMEMS.2018.2874231.

[10] J. Schulte, Z. Jiang, O. Sevim & O. E. Ozbulut, "Graphene-reinforced cement composites for smart infrastructure systems", The Rise of Smart Cities: Advanced Structural Sensing and Monitoring Systems **2022** (2022) 79. https://doi.org/10.1016/B978-0-12-817784-6.00008-4.

[11] D. B. Shinde, J. Brenker, C. D. Easton, R. F. Tabor, A. Neild & M. Majumder, "Shear assisted electrochemical exfoliation of graphite to graphene", Langmuir **32** (2016) 3552. https://doi.org/10.1021/acs.langmuir.5b04209

[12] L. Li, M. Wang, J. Guo, M. Cao, H. Qiu, L. Dai & Z. Yang, "Regulation of radicals from electrochemical exfoliation of a double-graphite electrode to fabricate high-quality graphene", Journal of Materials Chemistry C **6** (2018) 6257. https://doi.org/10.1039/c8tc01565a.

[13] Q. Zhou, Y. Lu & H. Xu, "High-yield production of high-quality graphene by novel electrochemical exfoliation at air-electrolyte interface" Materials Letters **235** (2019) 153. https://doi.org/10.1016/j.matlet.2018.10.016

[14] S. Yang, S. Brüller, Z. Wu, Z. Liu, K. Parvez, R. Dong, F. Richard, P. Samori, X. Feng & K. Müllen, "Organic Radical-Assisted Electrochemical Exfoliation for the Scalable Production of High-Quality Graphene", Journal of the American Chemical Society **137** (2015) 13927. https://doi.org/10.1021/jacs.5b09000.

[15] J. Liu, *Electrochemical Exfoliation Synthesis of Graphene" in Graphene-Based Composites for Electrochemical Energy Storage*, 2017, pp. 39–50. https://doi.org/10.1007/978-981-10-3388-9_2.

[16] L. Li, D. Zhang, J. Deng, J. Fang & Y. Gou, "Review—preparation and application of graphene-based hybrid materials through electrochemical xxfoliation", Journal of The Electrochemical Society **167** (2020) 086511. https://doi.org/10.1149/1945-7111/ab933b.

[17] L. Li, D. Zhang, J. Deng, Q. Kang, Z, Liu, J. Fang & Y. Gou, "Review—progress of research on the preparation of graphene oxide via electrochemical approaches", Journal of The Electrochemical Society **167** (2020) 155519. https://doi.org/10.1149/1945-7111/abbbc0

[18] M. Eredia, S. Bertolazzi, T. Leydecker, M. El Garah, I. Janica, G. Melinte, O. Ersen, A. Ciesielski & P. Samorì, "Morphology and Electronic Properties of Electrochemically Exfoliated Graphene", Journal of Physical Chemistry Letters **8** (2017) 3347. https://doi.org/10.1021/acs.jpclett.7b01301.

[19] J. H. Zhong, J. Zhang, X. Jin, J. Y. Liu, Q. Li, M. H. Li, W. Cai, D. Y. Wu, D. Zhan & B. Ren, "Quantitative correlation between defect density and heterogeneous electron transfer rate of single layer graphene", Journal of the American Chemical Society **136** (2014) 16609. https://doi.org/10.1021/ja508965w.

[20] T. C. Achee, W. Sun, J. T. Hope, S. G. Quitzau, C. B. Sweeney, S. A. Shah, T. Habib & M. J. Green, "High-yield scalable graphene nanosheet production from compressed graphite using electrochemical exfoliation", Scientific Reports **8** (2018) 1. http://dx.doi.org/10.1038/s41598-018-32741-3.

[21] Y. Hong, Z. Wang & X. Jin, "Sulfuric acid intercalated graphite oxide for graphene preparation", Sci. Rep. **3** (2013) 5. https://doi.org/10.1038/srep03439.

[22] H. Yu, B. Zhang, C. Bulin, R. Li & R. Xing, "High-efficient Synthesis of Graphene Oxide Based on Improved Hummers Method", Scientific Reports **6** (2016) 1. https://doi.org/10.1038/srep36143.

[23] C. Y. Su, A. Y. Lu, Y. Xu, F. R. Chen, A. N. Khlobystov & L. J. Li, "High-quality thin graphene films from fast electrochemical exfoliation", ACS Nano **5** (2011) 2332. https://doi.org/10.1021/nn200025p.

[24] F. Liu, C. Wang, X. Sui, M. A. Riaz, M. Xu, L. Wei, & Y. Chen, "Synthesis of graphene materials by electrochemical exfoliation: Recent progress and future potential", Carbon Energy **1** (2019) 173. https://dx.doi.org/10.1002/cey2.14

[25] J. M. Munuera, J. I. Paredes, M. Enterría, A. Pagán, S. Villar-Rodil, M. F. R. Pereira, J. I. Martins, J. L. Figueiredo, J. L. Cenis, A. Martínez-Alonso & J. M. D. Tascón, "Electrochemical Exfoliation of Graphite in Aqueous Sodium Halide Electrolytes toward Low Oxygen Content Graphene for Energy and Environmental Applications", ACS Applied Materials and Interfaces **9** (2017) 24085. https://doi.org/10.1021/acsami.7b04802.

[26] C. H. Chen, S. W. Yang, M. C. Chuang, W. Y. Woon & C. Y. Su, "Towards the continuous production of high crystallinity graphene via electrochemical exfoliation with molecular in situ encapsulation", Nanoscale **7** (2015) 15362. https://doi.org/10.1039/c5nr03669k.

[27] J. M. Munuera, J. I. Paredes, S. Villar-Rodil, M. Ayán-Varela, A. Martínez-Alonso & J. M. D. Tascón, "Electrolytic exfoliation of graphite in water with multifunctional electrolytes: En route towards high quality, oxide-free graphene flakes", Nanoscale **8** (2016) 2982. https://doi.org/10.1039/c5nr06882g

[28] A. Ambrosi & M. Pumera, "Electrochemically Exfoliated Graphene and Graphene Oxide for Energy Storage and Electrochemistry Applications" Chemistry - A European Journal **22** (2016) 153. https://doi.org/10.1002/chem.201503110.

[29] K. Parvez, Z. Wu, R. Li, X. Liu, R. Graf, X. Feng & K. Mullen, "Exfoliation of Graphite into Graphene in Aqueous Solutions ofInorganic Salts", American Chemical Society **136** (2014) 6083. https://doi.org/10.1021/ja5017156.

[30] C. H. Chuang, C. Y. Su, K. T. Hsu, C. H. Chen, C. H. Huang, C. W. Chu & W. R. Liu, "A green, simple and cost-effective approach to synthesize high quality graphene by electrochemical exfoliation via process optimization", RSC Advances **5** (2015) 54762. https://doi.org/10.1039/c5ra07710a.

[31] K. Parvez, R. Li, S. R. Puniredd, Y. Hernandez, F. Hinkel, S. Wang, X. Feng & K. Müllen, "Electrochemically exfoliated graphene as solution-processable, highly conductive electrodes for organic electronics", ACS Nano **7** (2013) 3598. https://doi.org/10.1021/nn400576v.

[32] X. Huang, S. Li, Z. Qi, W. Zhang, W. Ye & Y. Fang, "Low defect concentration few-layer graphene using a two-step electrochemical exfoliation", Nanotechnology **26** (2015) 105602. http://dx.doi.org/10.1088/0957-4484/26/10/105602

[33] P. Zhang, Q. Wang, Y. Fang, W. Chen, A. A. Kirchon, M. Baci, M. Feng, V. K. Sharma, & H. C. Zhou, *7 - Metal-organic frameworks for capture and degradation of organic pollutants. In: Metal-Organic Frameworks (MOFs) for Environmental Applications* Elsevier Inc., 2019, pp 203–29. https://dx.doi.org/10.1016/B978-0-12-814633-0.00009-0.

[34] X. Feng, X. Wang, W. Cai, S. Qiu, Y. Hu & K. M. Liew, "Studies on Synthesis of Electrochemically Exfoliated Functionalized Graphene and Polylactic Acid/Ferric Phytate Functionalized Graphene Nanocomposites as New Fire Hazard Suppression Materials" ACS Applied Materials and Interfaces **8** (2016) 25552. https://doi.org/10.1021/acsami.6b08373.

[35] Y. Lin, X. Sun, D. S. Su, G. Centi & S. Perathoner, "Catalysis by hybrid sp2/sp3 nanodiamonds and their role in the design of advanced nanocarbon materials" Chemical Society Reviews **47** (2018) 8438. https://doi.org/10.1039/c8cs00684a.

[36] S. Yang, A. G. Ricciardulli, S. Liu, R. Dong, M. R. Lohe, A. Becker, M. A. Squillaci, P. Samorì, K. Müllen & X. Feng, "Ultrafast Delami-

nation of Graphite into High-Quality Graphene Using Alternating Currents", Angewandte Chemie - International Edition **56** (2017) 6669. https://doi.org/10.1002/anie.201702076.

[37] H. Lee, J. Il Choi, J. Park, S. S. Jang & S. W. Lee, "Role of anions on electrochemical exfoliation of graphite into graphene in aqueous acids", Carbon N Y. **167** (2020) 816. https://doi.org/10.1016/j.carbon.2020.06.044.

[38] M. Wall, "The Raman Spectroscopy of Graphene and the Determination of Layer Thickness" Thermo scientific 170 (2011) 35. http://dx.doi.org/10.31399/asm.amp.2012-04.p035.

[39] N. Kure, I. H. Daniel, N. M. Hamidon, I. I. Lakin, B. U. Machu & E. J. Adoyi, "Effect of Time on the Syntheses of Carbon Nanotubes via Domestic Oven", Journal of the Nigerian Society of Physical Sciences **4** (2022) 59. https://doi.org/10.46481/jnsps.2022.355.

[40] L. G. Cançado, A. Jorio, E. H. M. Ferreira, F. Stavale, C. A. Achete, R. B. Capaz, M. V. O. Moutinho, A. Lombardo, T. S. Kulmala & A. C. Ferrari, "Quantifying defects in graphene via Raman spectroscopy at different excitation energies", Nano Letters **11** (2011) 3190. https://doi.org/10.1021/nl201432g.

[41] A. C. Ferrari, "Raman spectroscopy of graphene and graphite: Disorder, electron-phonon coupling, doping and nonadiabatic effects", Solid State Communications **143** (2007) 47. https://doi.org/10.1016/j.ssc.2007.03.052.

[42] A. C. Ferrari & D. M. Basko, "Raman spectroscopy as a versatile tool for studying the properties of graphene", Nature Nanotechnology **8** (2013) 235. https://doi.org/10.1038/nnano.2013.46.

[43] J. Bin Wu, M. L. Lin, X. Cong, H. N. Liu & P. H. Tan, "Raman spectroscopy of graphene-based materials and its applications in related devices", Chemical Society Reviews **47** (2018) 1822. http://dx.doi.org/10.1039/c6cs00915h.

[44] M. A. Pimenta, G. Dresselhaus, M. S. Dresselhaus, L. G. Cançado, A. Jorio & R. Saito, "Studying disorder in graphite-based systems by Raman spectroscopy", Physical Chemistry Chemical Physics **9** (2007) 1276. https://doi.org/10.1039/b613962k.

[45] Q. Wen, Z. Yu & R. Riedel, "The fate and role of in situ formed carbon in polymer-derived ceramics", Progress in Materials Science **109** (2020) 100623. https://doi.org/10.1016/j.pmatsci.2019.100623.

[46] N. Larouche & B. L. Stansfield, "Classifying nanostructured carbons using graphitic indices derived from Raman spectra", Carbon N Y **48** (2010) 620. http://dx.doi.org/10.1016/j.carbon.2009.10.002.

[47] H. Lee, J. Baek, K. S. Dae, S. Jeon & J. M. Yuk, "Hydrogen-Assisted Fast Growth of Large Graphene Grains by Recrystallization of Nanograins", ACS Omega **5** (2020) 31502. https://doi.org/10.1021/acsomega.0c02701.

[48] T. Majumder & S. P. Mondal, "Advantages of nitrogen-doped graphene quantum dots as a green sensitizer with ZnO nanorod based photoanodes for solar energy conversion", Journal of Electroanalytical Chemistry **769** (2016) 48. http://dx.doi.org/10.1016/j.jelechem.2016.03.018.

[49] S. Ullah, Q. Shi, J. Zhou, X. Yang, H. Q. Ta, M. Hasan, N. M. Ahmad, L. Fu, A. Bachmatiuk, & M. H. Rümmeli, "Advances and Trends in Chemically Doped Graphene", Advanced Materials Interfaces **7** (2020) 1. https://doi.org/10.1002/admi.202000999.

[50] P. T. Araujo, M. Terrones & M. S. Dresselhaus, "Defects and impurities in graphene-like materials", Materials Today **15** (2012) 98. http://dx.doi.org/10.1016/S1369-7021(12)70045-7.

[51] D. Savvas & G. Stefanou, "Determination of random material properties of graphene sheets with different types of defects", Composites Part B: Engineering **143** (2018) 47. https://doi.org/10.1016/j.compositesb.2018.01.008.